

Massachusetts Institute of Technology

POLYMER DEGRADATION RATE CONTROL  
OF  
HYBRID ROCKET COMBUSTION

by

David B. Stickler  
Kumar N.R. Ramohalli

September 1970

This Research Carried Out in the Space  
Propulsion Laboratory, M.I.T., in Cooperation  
with Lewis Research Center, NASA, under  
Grant NGL 22-009-383

FACILITY FORM 602

N72-13735  
(ACCESSION NUMBER)

143  
(PAGES)

CR-72-114  
(NASA CR OR TMX OR AD NUMBER)

(THRU)

(CODE)

(CATEGORY)

Reproduced by  
NATIONAL TECHNICAL  
INFORMATION SERVICE  
Springfield, Va. 22151

## ABSTRACT

Polymer degradation to small fragments is treated as a rate controlling step in hybrid rocket combustion. Both numerical and approximate analytical solutions of the complete energy and polymer chain bond conservation equations for the condensed phase are obtained. Comparison with inert atmosphere data is very good. It is found that the intersect of curves of pyrolysis rate versus interface temperature for hybrid combustors, with the thermal degradation theory, falls at a pyrolysis rate very close to that for which a pressure dependence begins to be observable. Since simple thermal degradation cannot give sufficient depolymerization at higher pyrolysis rates, it is suggested that oxidative catalysis of the process occurs at the surface, giving a first order dependence on reactive species concentration at the wall. Estimates of the ratio of this activation energy and interface temperature are in agreement with best fit procedures for hybrid combustion data. Requisite active species concentrations and flux are shown to be compatible with turbulent transport. Pressure dependence of hybrid rocket fuel regression rate is thus shown to be describable in a consistent manner in terms of reactive species catalysis of polymer degradation.

TABLE OF CONTENTS

	<u>Page</u>
ABSTRACT	i
TABLE OF CONTENTS	ii
LIST OF FIGURES	iii
NOMENCLATURE	iv
I. INTRODUCTION	1
II. THEORETICAL TREATMENT	4
A. Polymer Degradation - Analytical Treatment	4
B. Activation Energy Variation	10
C. Polymer Degradation - Numerical Integration	11
D. Comparison with Experiment	12
E. Oxidizer Transport in Turbulent Systems	16
III. CONCLUSIONS	21
APPENDIX A: VAPORIZABLE FRAGMENT SIZE CRITERIA	23
REFERENCES	28

LIST OF FIGURES

1. Turbulent Boundary Layer Combustion Format
2. Polymer Regression Rate Dependence on Free Stream Mass Velocity
3. Polymer Degradation Region Geometry
4. Dimensionless Variable Solution Curve
5. Calculated Polymer Pyrolysis Rate  
Analytic Solution, Activation Energy Constant
6. Calculated Polymer Pyrolysis Rate  
Numerical Solution for PMMA, with Varying Activation Energy
7. Polymer Pyrolysis Rate; PMMA  
Solid Lines - Varying  $E$ ,  $\alpha$  Solution
8. Turbulent Mixing and Reaction in Hybrid Boundary Layer

NOMENCLATURE

$A_0$	Avogadro's number	$[\text{gm-mole}^{-1}]$
B	kinetic rate frequency factor	$[\text{sec}^{-1}]$
C	specific heat of condensed phase	$[\text{cal/gm}^\circ\text{K}]$
D	Damköhler's Number	[0] Eq. 29
E	kinetic rate activation energy	$[\text{K cal/gm mole}]$
G	gas phase mass velocity, free stream	$[\text{gm/cm}^2 \text{ sec}]$
H	enthalpy required for bondbreaking to give monomer, per mass	$[\text{cal/gm}]$
$H_v$	heat of vaporization, per mole	$[\text{cal/gm mole}]$
hp	apparent heat of polymer pyrolysis	$[\text{cal/gm}]$
I	number of breakable bonds per unit mass	$[\text{gm}^{-1}]$
K	gas phase species concentration	[0]
$K_1$	polymer degradation constant	[0] Eq. 11
$K_2$	polymer degradation constant	[0] Eq. 11
$l$	oxidative degradation depth	[cm]
M	molecular weight	$[\text{gm/gm-mole}]$
N	number of monomer units per polymer chain (averaged)	[0]
n	number of monomer units defining specific polymer chain length	[0]
P	pressure	[atmospheres]
p	spatial gradient of temperature	[0] Eq. 11
$\dot{q}$	heat flux	$[\text{cal/cm}^2 \text{ sec}]$
R	universal gas constant	$[\text{cal/gm mole}^\circ\text{K}]$
Re <sub>x</sub>	Reynolds number based on axial position	[0]
$R_T$	turbulence time correlation function	[0]

$\dot{r}$	linear pyrolysis rate	[cm/sec]
T	temperature	[°K]
t	time	[sec]
$t_0$	turbulent mixing reference time	[sec]
U	gas velocity parallel with wall	[cm/sec]
$u'$	turbulent perturbation velocity	[cm/sec]
v	gas velocity perpendicular to wall	[cm/sec]
x	spatial coordinate normal to wall, in solid	[cm]
y	spatial coordinate normal to wall, in boundary layer	[cm]
$\delta$	boundary layer thickness	[sec]
$\tau$	temperature variable;	[0] Eq. 11
	characteristic time	[sec]
$\xi$	distance variable	[0] Eq. 11
$\Psi$	temperature variable	[0] Eq. 18
$\Theta_A$	activation energy parameter	$E/RT_w = [0]$
$\nu$	number density per mass	[gm <sup>-1</sup> ]
$\lambda$	polymer thermal conductivity	[cal/cm sec°K]
$\rho_F$	polymer density	[gm/cm <sup>3</sup> ]
$\rho_n$	gas phase density of fragment length n at wall	[gm/cm <sup>3</sup> ]

Subscripts

c	combustion chamber
e	boundary layer outer edge
i	initial
j	reference state for Clapeyron Equation
m	monomer
n	fragment length n monomer units
o	initial polymer state
ox	oxidizer, oxidative
th	thermal
w	wall, phase change interface

POLYMER DEGRADATION RATE CONTROL  
OF  
HYBRID ROCKET COMBUSTION

I. INTRODUCTION

The concept of hybrid combustion as a means of production of a working fluid for propulsion applications has been under consideration for a number of years. The earliest experimental work was carried out in Germany, where solid graphite was combusted with gaseous nitrous oxide ( $N_2O$ ).<sup>(1)</sup> Subsequently, Bartel and Rannie<sup>(2)</sup> at JPL studied combustion of graphite with air. In both cases, a circular port in the graphite carried the oxidizer gas, with turbulent transport of oxidizer to the solid wall the rate controlling step. The high ignition temperature requisite for graphite surface oxidation, and low linear regression rate obtainable, rendered these systems of little practical value.

More recently, polymeric fuels in combination with relatively concentrated oxidizers such as  $O_2$ ,  $N_2O_4$ ,  $F_2$ ,  $ClF_3$  have been studied. The major problem in such systems was found to be uniformity of fuel pyrolysis, and subsequent mixing of fuel and oxidizer to establish a flame zone. A number of combustor systems, differing essentially in the primary fluid flow field, have been investigated. The most highly developed system is based upon turbulent boundary layer combustion, as shown in Figure 1. Turbulent transport of oxidizer from the free stream, and of fuel from the polymer surface, result in a combustible mixture within the boundary layer. Heat transfer from the high temperature flame zone to polymer surface provides energy for pyrolysis. A model based upon turbulent transport as the primary rate control is well developed, primarily by Gilbert, Marxman, Woldridge, and Muzzy.<sup>(3,4,5)</sup> The basic prediction of this is that fuel linear regression rate varies with free stream mass velocity  $G$ , and is independent of pressure  $P_c$ . It can be expressed in the form

$$\dot{r} = G^{0.8} \quad (1)$$

The full form of this expression is found to predict quantitatively the behavior of many fuel-oxidizer systems, under low  $G$ , high  $P_c$  conditions. However, it is observed<sup>(6,7)</sup> that in high  $G$ , low  $P_c$  combustion situations, the fuel pyrolysis rate is lower than predicted, and, for very high  $G$ , appears independent of it, and dependent only on  $P$ . This behavior is shown quantitatively as Figure 2.

A number of physical explanations of this behavior have been proposed, and treated in the form of mathematical models.<sup>(8,9,10)</sup> These concepts include



flame zone broadening due to increased turbulence level, finite rate gas kinetics, and finite rate heterogeneous exothermic reaction. While some of these models can be made to fit experimental data fairly closely, they require physically unrealistic constants to do so.

The phase change of the fuel component implicit in all current hybrid systems has commonly been assumed to proceed at a rate directly proportional to the heat flux available to the surface, under steady state conditions. The constant of proportionality in this relation has not been considered as other than a constant. Both Rabinovitch<sup>(11)</sup> and Houser and Peck<sup>(12)</sup> have attempted to consider polymer behavior prior to vaporization explicitly. It is clear that the high molecular weight polymer must degrade into lower molecular weight fragments in order to vaporize. Houser and Peck<sup>(12)</sup> assumed monomer to leave the surface. Rabinovitch<sup>(11)</sup> attempted to define a "critical fragment size" from energy utilization considerations. Neither gave an adequate treatment of the energy equation in the condensed phase, or considered volatilization adequately.

Some studies into polymer degradation and pyrolysis products have been carried out by use of arc imaging furnaces.<sup>(13)</sup> It is found that fragments collected as gas at temperatures of interest range from one to several monomer units in size. Since thermal degradation in the gas phase, near the imaging region, will also have occurred, the concept of vaporizing fragment size greater than monomer is well established, although a quantitative local number for the polymer surface has not been obtained. Fragment size is also strongly dependent upon the specific polymer treated.

The work undertaken here was initiated to investigate the effect of gas phase oxidizer on polymer pyrolysis, as a rate controlling step in hybrid combustion. It is hypothesized that catalytic oxidizer attack will result in an increase in polymer fragmentation rate at the surface, and hence in an increase in possible vaporization rate. A three part problem in combustion then must be considered. The thermal degradation of polymer proceeds in the condensed phase. Transport of oxidizer through a combustion zone to the fuel surface must be considered in the gas phase. Finally, matching conditions at the phase change interface must be established and satisfied.

It is shown analytically in Section II that thermal degradation of polymethylmethacrylate (PMMA) proceeds at a sufficient rate to permit low regression rate hybrid combustion, as occurs at low free stream mass velocity. It is not by itself sufficient to give high linear regression rates such as are observed

in the pressure sensitive hybrid combustion region. It is hypothesized that an oxidative bond breaking mechanism acts at the polymer surface, at a rate proportional to the concentration of oxidizer at the wall. The estimated ratio of activation energy<sup>(14)</sup> to wall temperature for this step is found equal to that obtained by Wooldridge and Marxman<sup>(10)</sup> as best fit for their treatment. Oxidizer concentration and flux at the wall requisite for attack at the necessary rate are calculated. The former is found to be that commonly measured<sup>(15,16)</sup>, and the latter orders of magnitude lower than the maximum possible in the turbulent boundary layer-flame zone flow field. Data on the turbulent mixing and combustion of free jets<sup>(17,18)</sup> indicates that reaction proceeds at the interfaces of "eddies" of fuel and oxidizer. Furthermore, there is a finite flux of unreacted oxidizer through such a combustion region, due to the low rate of molecular diffusion, required for combustion, relative to turbulent transport rate. A mechanism does therefore exist for oxidizer supply to polymer surface.

## II. THEORETICAL TREATMENT

### A. Polymer Degradation - Analytical Treatment

The chemical structure change inherent in the vaporization of a polymeric material at finite pressures proceeds at a finite rate in the solid phase material. A number of chemical bonding changes may occur during polymer degradation. For a straight chain structure such as PMMA, or one with few cross links relative to straight chain links, the most interesting process prior to vaporization is random thermal bond breaking.<sup>(11)</sup> A broken polymer bond may in some cases serve as an initiation point for very rapid local "unzipping" of the chain. This behavior is reported with particular reference to PMMA.<sup>(13,19)</sup> If this is in fact the physical situation, one must consider essentially all the polymer to vaporize as monomer, rather than as larger fragments as observed for polystyrene.<sup>(13)</sup> In either case, the kinetically controlled polymer degradation process is responsible for breaking a fraction of the straight chain bonds initially present. The remainder either break rapidly upon initiation, or do not break prior to fragment vaporization. A local fragment size, notably a final chain length at the wall is then a useful mathematical concept for both situations, subject to proper physical interpretation.

The rate of thermal bond breaking in a polymer can be expressed in an Arrhenius format as

$$\frac{dI}{dt} = -I B e^{-E/RT} \quad (2)$$

where  $I$  is the number of breakable bonds present per unit mass at time  $t$ . Initially the polymer has a mean molecular weight of  $M_0$ , and a constant monomer molecular weight of  $M_m$ , so that the number of monomer units per polymer chain is

$$N_0 = M_0 / M_m \quad (3)$$

and the number of breakable bonds is  $N_0 - 1$ . Normally,  $N_0$  is a sufficiently large number that

$$N_0 - 1 \approx N_0 \quad (4)$$

However, when polymerization is approaching completion, this approximation is not valid. The number of breakable bonds per mass follows simply from the above as

$$I = \frac{N - 1}{N} \frac{A_0}{M_m} \quad (5)$$

and the fraction of breakable bonds present, relative to the initial number, is

$$\frac{I}{I_0} = \frac{N - 1}{N} \frac{N_0}{N_0 - 1} = \frac{N - 1}{N} \quad (6)$$

Steady state degradation and pyrolysis of a fuel material can be represented in the condensed phase by the well established energy equation

$$\rho_F \dot{r} \frac{d}{dx} (cT) + \frac{d}{dx} (\lambda \frac{dT}{dx}) = \frac{I}{I_0} H \rho_F B e^{-E/RT} \quad (7)$$

where  $H$  is the energy required for complete depolymerization of one unit mass of polymer, initially of chain length  $N_0$ , and the sign conventions are indicated on Figure 3. The condensed phase specific heat and thermal conductivity are indicated as being dependent on  $x$  in this formulation. This follows from the variation of temperature and mean molecular weight, or fragment size, with position. It is assumed in the analytical treatment that both  $c$  and  $\lambda$  may be represented as appropriate average quantities.

The appearance of a fractional number density of breakable polymer bonds on the right hand side of the energy equation requires the writing of a relation analogous to a chemical species equation. If it is assumed that convection at a mass rate  $\rho_F \dot{r}$  is the sole means of spatial species transport, Equation (2) can be rewritten as

$$\rho_F \dot{r} \frac{d}{dx} \left( \frac{I}{I_0} \right) = \frac{I}{I_0} \rho_F B e^{-E/RT} \quad (8)$$

Nondimensionalization of Equations (7) and (8) by use of the definitions given

below (Equation 11) leads to .

$$p + \frac{dp}{d\tau} = \frac{I}{I_0} K_1 e^{-E/R [(T_w - T_i)\tau + T_i]} \quad (9)$$

$$p \frac{d}{d\tau} \left( \frac{I}{I_0} \right) K_1 K_2 e^{-E/R [(T_w - T_i)\tau + T_i]} \quad (10)$$

where

$$\tau = \frac{T - T_i}{T_w - T_i}$$

$$\xi = \frac{\rho_F \dot{r} c}{\lambda} x$$

$$p = \frac{d\tau}{d\xi} \quad (11)$$

$$K_1 = \frac{\lambda H B \rho_F}{(\rho_F \dot{r} c)^2 (T_w - T_i)}$$

$$K_2 = \frac{c(T_w - T_i)}{H}$$

This treatment eliminates all explicit spatial dependence in the problem, simplifying both the analysis and the boundary conditions, with no loss in useful information. It is clearly analogous to the approach taken in laminar flame propagation theory.

Multiplying Equation (9) by  $K_2$  and subtracting from (10), there results

$$\frac{d}{d\tau} \left( \frac{I}{I_0} \right) = \left( 1 + \frac{dp}{d\tau} \right) K_2 \quad (12)$$

with initial conditions deep within the polymer;

$$\begin{aligned} x \rightarrow \infty : \quad \tau &\rightarrow 0 \\ p &\rightarrow 0 \\ I/I_0 &\rightarrow 1 \end{aligned}$$

This integrates to

$$\frac{I}{I_0} = 1 + (\tau + p) K_2 \quad (13)$$

Combined with the energy equation, this gives

$$p + p \frac{dp}{d\tau} = [1 + (\tau + p) K_2] K_1 e^{-E/R} [(T_w - T_i) \tau + T_i] \quad (14)$$

The most useful result to be obtained from this equation is an eigenvalue for the constant  $K_1$ , so that a linear regression rate for the polymer, as a function of wall temperature and degree of depolymerization at the wall, may be obtained. To approximate this analytically, it is most useful to treat two limiting cases, one applying well within the polymer, and the other in the region near the surface. The former region has  $\tau < 1$ , and the right hand side of Equation (14) assumed negligible relative to conductive and convective rates.

The form results

$$1 + \frac{dp}{d\tau} = 0$$

with the conditions at

$$\begin{aligned} x \rightarrow \infty : \tau &\rightarrow 0 \\ p &\rightarrow 0 \end{aligned}$$

so that

$$p = -\tau ; \quad \tau < 1 \quad (15)$$

Referring back to the dimensionless spatial coordinate  $\xi$ , this gives

$$\tau = e^{-\xi} ; \quad \tau < 1, \xi > 0 \quad (16)$$

A curve of the gradient  $p$  versus  $\tau$  is sketched as Figure 4. As  $\tau \rightarrow 1$ , it is necessary that the physical slope of  $\tau$  increase in absolute value, to account for the heat required for a finite rate of depolymerization near the surface. The quantity  $p$  then approaches a value  $p_w < -1$  as  $\tau$  approaches 1. This is obtainable from the physical requirement that at the surface, conductive heat transfer rate into the polymer be equal to the total energy utilization rate within the polymer. The equation follows as

$$-\lambda \left. \frac{dT}{dx} \right|_w = \rho_F \dot{x} \left[ c(T_w - T_i) + H \left( 1 - \frac{T_w}{T_o} \right) \right]$$

This is nondimensionalized by use of Equation (11) to give

$$p_w = - \left[ 1 + \frac{1}{K_2} \left( 1 - \frac{T_w}{T_o} \right) \right] \quad (17)$$

The same result is directly obtainable as the wall limit of Equation (13), but with less obvious physical origin.

Solution of Equation(14) in the region of high thermal degradation rate leads to an eigenvalue  $K_1$ . This proceeds by the variable changes

$$\psi \equiv \frac{E}{RT_w} \frac{T_w - T_i}{T_w} (1 - \tau) = \theta_\Delta \frac{T_w - T_i}{T_w} (1 - \tau)$$

$$\eta = p + \tau \quad (18)$$

to give

$$\frac{d\eta}{d\psi} \frac{1 - \eta - \psi \frac{T_w}{T_w - T_i} \frac{1}{\theta_\Delta}}{1 + K_2 \eta} = \frac{K_1}{\theta_\Delta \frac{T_w - T_i}{T_w}} e^{-\frac{\theta_\Delta}{1 - \psi/\theta_\Delta}}$$

The term in  $\psi$  on the left side is readily seen to be very small in the wall region, and to zeroth order is considered negligible. The convective enthalpy flux is thus dropped in the high depolymerization rate region near the wall. Also, the denominator of the exponential is expanded. There then results the form

$$K_2 \frac{1 - \eta}{1 + K_2 \eta} \frac{d\eta}{d\psi} = \Lambda e^{-\psi} \quad (19)$$

where

$$\Lambda = \frac{K_1 K_2 \cdot e^{-\theta_\Delta}}{\theta_\Delta \frac{T_w - T_i}{T_w}} \quad (20)$$

This has the boundary conditions:

polymer interior	phase change interface
$\psi \rightarrow \infty$	$\psi = 0$
$\eta \rightarrow 0$	$\eta = p_w + 1$

Integration and use of Equations (17) and (6) results in the following expression for the eigenvalue  $\Lambda$ .

$$\Lambda = \left(1 + \frac{1}{K_2}\right) \ln \frac{N_w}{N_w - 1} - \frac{1}{K_2 N_w} \quad (21)$$

It is thus shown that the eigenvalue defined is dependent only on the fragment size at the wall, and the thermal parameter  $K_2$ . To return to the physical plane,  $K_1$  and  $K_2$  are introduced explicitly in Equations (20) and (21). The linear pyrolysis rate is found to be

$$\dot{r} = \frac{\lambda B}{\rho_F c} \frac{e^{-E/RT_w}}{\frac{E}{RT_w} \frac{T_w - T_i}{T_w}} \frac{1}{\left[\frac{H}{c(T_w - T_i)} + 1\right] \ln \frac{N_w}{N_w - 1} - \frac{H}{c(T_w - T_i)N_w}} \quad (22)$$

The dependence of  $\dot{r}$  on the phase change interface temperature  $T_w$  is dominated by the exponential term. This expression is most readily plotted as the logarithm of the burning rate as a function of inverse wall temperature, as done for polymethyl methacrylate on Figure 5. Thermal diffusivity of the degrading condensed phase, and activation energy, are held constant, independent of local temperature and degree of depolymerization. Numerical treatments are employed below to introduce such "real material" effects. The mean effective fragment size  $N_w$  is taken as a parameter of the curves. Linear pyrolysis rate, at a given wall temperature, is seen to increase with increasing  $N_w$ . This corresponds to higher pyrolysis rate for a less completely degraded vaporizing material. Requiring



that  $N_w = 1$  implies that monomer is produced, by thermal bond breaking, and results in a zero net pyrolysis rate. This is a consequence of the approximation in the bond conservation equation, to the effect that no species diffusion occurs. This assumption is not valid physically, but is found to be unimportant for the fragment sizes of interest in the following discussion.

### B. Activation Energy Variation

It is found empirically<sup>(20)</sup> that the absolute rate of PMMA thermal degradation decreases as the degree of depolymerization increases. This has been interpreted as being due to preferential breaking of weaker bonds [e.g. - C - O - C - ] initially, so that subsequent thermal degradation requires breaking of progressively stronger chain bonds. A variation of activation energy with degree of depolymerization, in the present notation  $I/I_0$ , is thus suggested.<sup>(20)</sup> It is expressed as

$$E = E_0 + \Delta E \left(1 - \frac{I}{I_0}\right) \quad (23)$$

The primary effect of the variation of activation energy with degree of thermal depolymerization is obtained in the overall regression rate, as a function of mean effective fragment size,  $N_w$ . Decreasing  $N_w$  requires a higher mean activation energy in Equation (20), so that  $\dot{r}$  decreases both due to the requirement that more polymer bonds be broken, and the effect of a lower absolute bond breaking rate. This latter is handled in the numerical integration of Equation (14) by direct application of Equation (23), with reference to local chain length. The effect is clearly unimportant for  $N > 10$ , or equivalently, within the cooler polymer regions.

### C. Polymer Degradation - Numerical Integration

The cases treated analytically lead to an approximation to numerically correct results for a pyrolysis rate, and to a useful form of the energy equation for numerical integration. This is rewritten here as

$$p + p \frac{dp}{d\tau} = 1 + (\tau + p)K_2 K_1 e^{-E/R[(T_w - T_i)\tau + T_i]}$$

As in the analytical treatment, this is handled numerically as a boundary value problem, with  $K_1$  treated as an eigenvalue. The boundary conditions are readily cited from the previous section as

$x = 0$ ; phase change interface

$\tau = 1$

$$p = - \left[ 1 + \frac{1}{K_2} \left( 1 - \frac{I_w}{I_o} \right) \right]$$

$x \rightarrow \infty$ ; undisturbed polymer

$\tau = 0$

$p = 0$

A stepwise integration procedure is employed, running from the phase change interface to the  $\tau = 0$  condition. Iteration on the parameter  $K_1$  leads to satisfaction of the boundary value  $p = 0$  at  $\tau = 0$ . The physical data input to this treatment are the phase change interface temperature  $T_w$ , and mean effective fragment size, as well as  $T_i$  and polymer characteristics. There result curves of  $\dot{r}$  as a function of  $T_w^{-1}$ , with  $N_w$  as a parameter. The results for PMMA are given as Figure 6, with a constant thermal diffusivity case indicated by dashed lines, and the same results corrected for a varying diffusivity by the solid lines. This correction is simply a ratio, defined as

$$\frac{\dot{r}(\alpha \text{ variable})}{\dot{r}(\alpha @ 300^\circ\text{K})} = \left[ \frac{\alpha(T_w)}{\alpha(300^\circ\text{K})} \right]^{1/2}$$

where the  $\alpha$  variation is taken from data in reference 22 as a linear function of  $T_w$ , through known points.

Direct comparison of the constant thermal diffusivity lines of Figure 6 with the analytical results of Figure 5 is somewhat misleading, due to the use of a varying activation energy for the numerical calculation. At larger vaporizing fragment size, the curves are quite similar. Smaller  $N_w$  leads both to a higher slope of the  $\dot{r}$  vs  $T_w^{-1}$  lines ( $\propto E^{1/2}$ ) and a lower absolute  $\dot{r}$  than for the analytic case. However, for any given set of constant parameters, it is found that the analytic and numerical solutions agree within a few percent. In subsequent discussions, the variable  $E$  and a numerical case is employed for comparison with PMMA pyrolysis and combustion data.

#### D. Comparison with Experiment

There are two classes of experimental data with which the above treatment of polymer degradation can usefully be compared. These are data taken in chemically inert, and in reactive atmosphere. The former bear some close resemblance to the predictions of the thermal degradation theory. The latter lead to the concept of oxidative depolymerization as a pressure sensitive mechanism in hybrid combustion.

The variation of regression rate with surface temperature for thermal degradation of PMMA, and of  $\dot{r}$  with  $T_w$  as obtained from hybrid combustion measurements, are plotted on Figure 7. Also indicated are several other experimental points. The work of Chaiken et al.<sup>(21)</sup> was done with a hot plate system, at an effective pressure of 2.77 atmospheres. The close fit of this theory with their data, in terms of slope, is apparent. The mean effective fragment size giving best fit is reasonable, independent of interpretation. A mean unzipping length of four to ten monomer units for every thermal initiation site is in agreement with free

radical unzipping mechanisms. Vapor pressure equilibrium is also a feasible criterion. The line given on Figure 7 as a vapor pressure criterion\* is obtained by application of the Clapeyron equation to straight chain hydrocarbon data, and assumes a constant heat of vaporization per unit mass of the material in question. A curve of  $N_w$  against the  $T_w$  required for 2.77 atmospheres vapor pressure is obtained, and matched with the  $N_w - T_w$  pyrolysis rate lines. The curve resulting is of the same shape as the data points given by Chaiken. Choice of a reference pressure dependence on fragment size more closely approximating the (unknown) behavior of short chain methyl methacrylate could perhaps improve the matching. Present data neither confirms nor refutes the concept of a vapor pressure equilibrium. Aside from gas phase composition measurements for various pyrolyzing polymers, there appears no grounds for choice between these hypotheses.

Combustion data are given by McAlevy et al.<sup>(22)</sup> for what appears to be effectively a stagnation point laminar boundary layer situation. These points parallel trends for turbulent boundary layer combustion quite closely, although at a higher wall temperature. Also, if extrapolated, they intercept data by McAlevy and Hansel<sup>(23)</sup> from porous plug burner experiments. A distinct difference in slope between the curves for thermal degradation, and the data for pyrolysis in reactive environments, including hybrid combustion boundary layers, is apparent.

Below the intercept of hybrid data with the thermal degradation curve, the polymer thermal degradation rate is sufficient to allow the observed hybrid combustor linear regression rates. The overall rate controlling process should then be heat transfer from gas to condensed phase. Polymer regression rates greater than the intersect rate require wall temperatures much higher than observed in the cited experiments, if thermal degradation is to provide adequate depolymerization. It is also observed by comparison with Figure 2 that polymer regression rate at this intersect is close to that for which regression rate

---

\* See Appendix A for more complete discussion.

pressure sensitivity becomes apparent, as a departure from the simple laminar and turbulent heat transfer situations.

Since simple thermal degradation does not lead to bond breaking rates sufficient for the observed high regression rates with any reasonable effective fragment size or wall temperature, it is clear that another mechanism of polymer de-radation must exist. The pressure dependent behavior exhibited leads immediately to the suggestion that a reactive gas phase component is involved. There are two distinct classes of chemical species which are present in an hybrid boundary layer and which can affect catalytically polymer degradation. These are unreacted oxidizer, and radicals present in equilibrium in a flame zone. Only the former may be expected to diffuse to the phase change interface through a "laminar sublayer" flow region.

The conclusion of McAlevy and Hansel<sup>(23)</sup> that oxidative attack is irrelevant in PMMA degradation was based upon tests for which the minimum  $O_2$  concentration was 9 mole percent, appreciably greater than necessary for oxidative attack, and sufficient to mask the effect of any of the additives employed by them. The thermal polymer degradation treatment given here suggests that significant oxidizer attack was involved in all such pyrolysis experiments, with pressure dependence appearing only at pyrolysis rates high enough to consume a significant fraction of the available oxidizer. This interpretation is reinforced by comparison with data for pressure dependent combustion of PMMA-Oxygen in a laminar flow system. There is close quantitative agreement between the pyrolysis rate at which pressure dependence is initially observed, and the intersect of hot plate (inert atmosphere) data with that of McAlevy and co-workers, as indicated by Figures 2 and 7.

The effect of oxidative degradation is assumed confined to a planar region near the phase change interface. As a first estimate, this region is assumed thin compared with that for which thermal degradation is important. The rate of oxidative

bond breaking is modeled in conventional fashion as an Arrhenius rate multiplied by relevant concentrations. The number density of breakable bonds follows from the thermal degradation treatment as that required for the assigned  $\dot{r}$  and  $T_w$ . Oxidizer concentration within this region is taken to be proportional to its partial pressure as gas at the wall. A bond breaking rate follows as

$$\frac{dI}{dt} = -I_{w,th} P_{ox} B_{ox} e^{-E_{ox}/RT_w}$$

A characteristic stay time for polymer within this region is

$$t_{ox} = \ell/\dot{r}$$

where  $\ell$  is the assumed thickness of the oxidative degradation region. Within this time period, the number of bonds broken per unit mass of material is approximately

$$\Delta I = I_{w,th} P_{ox} B_{ox} e^{-E_{ox}/RT_w} t_{ox}$$

Some numerical estimates are readily obtained from this. As a worst case, the ratio  $\Delta I/I_{w,th}$  may be approximately 0.9. From measurements in hybrid systems, (15,16) the molar concentration of oxidizing species at the wall is approximately one percent. Activation energy for oxidative polymer degradation, and the relevant frequency factor, are less well established. However, experimental measurements of polymer ignition in reactive atmospheres may provide an upper bound on  $E_{ox}$ . Anderson and Brown<sup>(14)</sup> report  $E_{ox}$  to be between 5 and 10  $K_{cal}$ . The frequency factor is taken to be  $10^{10} \text{ sec}^{-1}$ . These assumptions lead to the requirement that

$$P_c t_{ox} \sim 13 \cdot 10^{-7} \text{ atm sec}$$

Choice of a pressure of 5 atmospheres and  $\dot{r} \sim 1 \text{ m.m. per second}$  gives as a minimal depth

$$\ell \sim 2 \cdot 10^{-8} \text{ cm}$$

which is consistent with oxidative attack over a depth characterized by a few monomer unit lengths. Increased combustion pressure implies a shallower required degradation region, or equivalently, more complete degradation, and hence higher regression rate. In this limit, polymer degradation rate can then become sufficiently high that the effective pyrolysis rate control is by heat transfer, so that the simpler transport model prediction is approached.

The flux of oxidizer required for this degradation mechanism can be approximated as a worst case by assuming a single atom of oxidizer per monomer unit vaporizing. This leads to the approximate result

$$\dot{m}_{\text{ox}} \left( \frac{\text{gm}}{\text{cm}^2 \text{sec}} \right) \sim 0.05 \dot{r} \left( \frac{\text{cm}}{\text{sec}} \right)$$

as a maximum flux requirement for PMMA. Turbulent transport without reaction to a perfect sink wall can give transport rates an order of magnitude greater than this. It can therefore be suggested that adequate oxidizer transport may exist to permit the hypothesized catalytic polymer degradation at observed rates.

#### E. Oxidizer Transport in Turbulent System

Calculation of oxidizer flux from free stream to wall, through the hybrid combustor turbulent boundary layer, is clearly a complex problem. However, an argument regarding the physical existence and approximate magnitude of such a flux can be given in simple fashion. Both spatial transport of oxidizer, and destruction of it by chemical reaction, proceed at any given locus in the boundary layer. The former process is rate controlled by the local turbulent transport. The chemical reaction process presupposes molecular scale mixing between oxidizer and fuel. Within a local mixed region combustion proceeds at a finite rate. Such a mixed region is necessarily small in thickness relative to large scale turbulent eddies, but is assumed very large compared with molecular mean free

paths. Consideration of relative rates of oxidizer turbulent eddy dissipation, and local chemical reactions, leads to a local Damköhler number variation which taken with an approximate turbulent mixing model is consistent with the existence of a finite oxidizer concentration in the region of the polymer surface.

A gross approach to a maximum local rate of turbulent mixing is here based upon the standard time correlation function for homogeneous, isotropic turbulence.

$$R_T = e^{-t/t_0} \quad (24)$$

The local time rate of loss of correlation is therefore

$$-\frac{dR_T}{dt} = +\frac{1}{t_0} e^{-t/t_0}$$

The reference time scale  $t_0$  may be related to the boundary layer geometry as

$$\text{Mixing Length} = \sqrt{u'^2} \int_0^{\infty} R_T dt = \sqrt{u'^2} t_0$$

Assuming mixing length to be on the scale of the largest eddy, which may itself approximate the local boundary layer thickness  $\delta$ , the reference time is found to be

$$t_0 = \delta (u'^2)^{-1/2} \quad (25)$$

The time a fluid element, has been subject to turbulent transport and mixing within the boundary layer is approximately its free stream travel time from the leading edge of the boundary layer. For a given  $x, y$  position, this corresponds to

$$t = \frac{x}{u_e} \frac{\delta - y}{\delta} \quad (26)$$

The local characteristic mixing time, as determined by loss of large scale turbulent eddy identity can therefore be written



$$\tau_{\text{mix local}} = \frac{\delta}{(\overline{u'^2})^{1/2}} \exp - \left[ \frac{x}{\delta} \left( 1 - \frac{y}{\delta} \right) \frac{(\overline{u'^2})^{1/2}}{u_e} \right] \quad (27)$$

where the velocity ratio can be treated as a turbulent intensity level in the boundary layer. Local boundary layer thickness ( $\delta$ ) for the hybrid system has been treated by Marxman<sup>(24)</sup> and expressed as

$$\frac{\delta}{x} = \left[ \frac{0.0281}{I} (1 + B) \ln \frac{1 + B}{B} \right]^{0.8} R_{e_x}^{-0.2}$$

where

$$I = \frac{7(1 + \frac{13}{10}B + \frac{4}{11}B^2)}{72(1 + \frac{B}{2})^2}$$

A valid conceptual model for the local time scale of chemical reaction is not readily available for this particular case. One can write an Arrhenius rate expression, as will be done here, for the combustion process. However, this implies the existence of a continuous flame zone, with a definable temperature. Discrete localized reaction zones might be more accurately considered rate controlled by local ignition kinetics. Use of the Arrhenius model with a temperature equal to the local time averaged temperature of the fluid must then be considered a first approximation. It may, however, be conservative in terms of overall oxidizer transport. Assuming that some reference conditions are known, one can write

$$\tau_{\text{reaction}} \sim \tau_{\text{ref}} \exp \frac{E}{R} \left[ \frac{1}{T} - \frac{1}{T_{\text{ref}}} \right] \quad (28)$$

A Damköhler group may be formed from these chemical and mixing times, and written as

$$D = \left[ \frac{\tau_{\text{reaction}}}{\tau_{\text{mix}}} \right]_{\text{local}}$$

$$D = \frac{\tau_{\text{ref}} \exp \frac{E}{R} \left[ \frac{1}{T} - \frac{1}{T_{\text{ref}}} \right]}{\frac{\delta}{\sqrt{\overline{u'^2}}} \exp - \left[ \frac{x}{\delta} \left( 1 - \frac{y}{\delta} \right) \frac{\sqrt{\overline{u'^2}}}{u_e} \right]} \quad (29)$$

In the region between the time averaged visible flame zone and the wall, the value of  $D$  can be taken as an approximate measure of the survival of oxidizer in a homogeneous environment. For a locus with  $D$  large, one expects the existence of a finite local homogeneous oxidizer concentration. In particular, it is suggested that oxidizer diffused through the turbulent flame zone as discrete eddies may survive in a homogeneous mixture in the sub-flame region, and diffuse in normal fashion toward the wall. The maximum reasonable local concentration of oxidizer in the region of small  $D$  is described by the local correlation equation (24). With equations (25) and (26), one finds

$$\sim \exp - \left[ \frac{x}{\delta} \left( 1 - \frac{y}{\delta} \right) \frac{\sqrt{u'^2}}{u_e} \right] \quad (30)$$

The above equations can be compared with data taken from hybrid boundary layer simulator measurements. In particular, the hydrogen-air experiment reported by Wooldridge and Muzzy,<sup>(25)</sup> with flame speed measurements by Rosenfeld and Sugden<sup>(26)</sup> form a numerical basis. The corresponding chemical reaction time scale is written as

$$\tau_{\text{chem}} \sim 1.25 \cdot 10^{-5} \exp \left[ 32500 \left( \frac{1}{T} - 0.000786 \right) \right] \text{ [sec]}$$

and the mixing time scale

$$\tau_{\text{mix}} \sim 0.067 \exp \left[ 4.36 \left( 1 - \frac{y}{\delta} \right) \right] \text{ [sec]}$$

The Damköhler group is therefore

$$D \sim \frac{19 \cdot 10^{-5} \exp \left[ 32500 \left( \frac{1}{T} - 0.000786 \right) \right]}{\exp \left[ -4.36 \left( 1 - \frac{y}{\delta} \right) \right]}$$

and the local concentration of unmixed oxidizer

$$\frac{K_{\text{ox}}}{K_{\text{ox}_e}} \sim \exp - \left[ 4.36 \left( 1 - \frac{y}{\delta} \right) \right]$$

These are plotted on Figure 8, together with experimental oxidizer concentration measurements given in reference 25. The experimental points are seen to remain close to free stream oxidizer concentration, and well above the correlation line, for the boundary layer region above the flame zone. As the calculated  $D$  decreases through unity, however, measured concentration of oxygen drops toward that predicted by the correlation line. In the region close to the wall, finite oxygen concentrations remain observable, consistent with a finite eddy transport probability and large local Damköhler number. These observations simply reinforce the necessity of careful treatment of such initially unmixed turbulent flames.

### III. CONCLUSIONS

The combustion process in a hybrid rocket is well known to exhibit a positive pressure dependence, in regimes of high free stream mass flow. This effect is most clearly manifested as a lower polymer fuel pyrolysis rate at low pressures than is predicted by heat transfer analysis, or observed at high pressures. Both chemical kinetic steps in the gas phase heat release process, and heterogeneous exothermic mechanisms have been postulated as explanatory of this phenomenon. The former appears not to take full account of the basic structure of a turbulent flame zone, and the latter to require much higher oxidizer concentration at the wall than is observed experimentally.

This study is concerned with the kinetics of polymer degradation, specifically PMMA, as a prime rate controlling step in pyrolysis. It is found analytically that linear pyrolysis rate, as a function of wall temperature, exhibits the same slope as hot plate pyrolysis data, and matches it quantitatively if it is assumed that a single thermal chain rupture or initiation results in elimination of six monomer units. In terms of the degradation kinetic rate, it is inconsequential whether these are considered a six unit chain, two trimers, or six individual monomer units. The pyrolysis rate curve for an effective fragment size of six intersects both laminar and turbulent combustion data for  $\dot{r}$  versus  $1/T_w$  at regression rates quantitatively quite close to those for which pressure sensitivity is observed for the respective flow regimes. The hypothesis follows that catalytic oxidative attack is responsible for the excess of polymer degradation required for high pyrolysis rates at observed hybrid combustor wall temperatures, relative to that due to thermal degradation. Such a mechanism gives pyrolysis rates increasing with oxidizer concentration at the wall, until a pyrolysis rate corresponding to the heat transfer limit is reached. The requisite oxidizer concentration at the wall is found to be comparable with measured values, and the maximum usable

flux is compatible with turbulent transport through a reaction zone. The thickness of the condensed phase region which must be subject to such attack is found to be equivalent to or less than a few monomer unit lengths, so that one can in fact speak of a surface degradation process.

Comparison of the hypothesized mechanism with available data yields no qualitative disagreement. In the specific case of PMMA - oxygen combustion, agreement between theory and experiment approaches quantitative.

Numerous areas of incomplete knowledge are evident in this study. These most notably include details of polymer fragmentation, and kinetics of oxidative degradation. The former is important with respect to quantitative matching conditions between gas phase and surface, the latter for prediction of actual pyrolysis rate under pressure dependent conditions. Also, knowledge of combustion and transport processes in a turbulent boundary layer, while clearly adequate for time averaged heat transfer estimates, is not sufficient for an understanding of free stream species transport through a combustion region to the wall. This last area is subject to experimental study by the present investigators.

APPENDIX AVAPORIZABLE FRAGMENT SIZE CRITERIA

The treatment given above indicates that the linear regression rate of a polymer is closely coupled with the mean number of monomer units associated with a polymer chain bond rupture. This number may be interpreted in two ways. As is implicit in the preceding sections, the number of monomer units may be treated as a single vaporizing fragment of chain length  $N_v$  for many polymers. This is the interpretation originally suggested by Rabinovitch.<sup>(11)</sup> Alternatively, one can conceive of the point rupture of a PMMA chain as the initiation of a very rapid local degradation process resulting in a number of individual monomer units. This interpretation was put forward by Madorsky,<sup>(19)</sup> and further discussed by Nagler.<sup>(13)</sup> For an effective fragment size at the phase change interface of several monomer units, both these interpretations are equivalent with respect to the kinetic thermal degradation treatment of Section II, A and B. Polymer pyrolysis kinetic rate at an assigned  $T_w$  is dependent not on the true fragment size vaporizing, but on the number of thermal depolymerization points involved.

The chemical structure of pyrolysis products is however of dominant import with respect to matching conditions at the phase change interface. Both the fragment vapor pressure relative to combustion chamber pressure, and the effective heat of pyrolysis of the polymer are dependent upon this. Both of the possible situations cited above are discussed in the following paragraphs.

It is first assumed that at the phase change interface, the gas phase is composed essentially of only fuel molecules, with a distribution of fragment sizes  $n < 1$  represented, and that they are in vapor pressure equilibrium with the condensed phase, at the interface temperature. The sum of the partial pressures

of the various fragment sizes must then equal the local static pressure  $P_c$ , or

$$P_c = \sum_n P_n(T_w) \quad (31)$$

It is useful to approximate the temperature dependence of species vapor pressure by means of the Clapeyron equation, viz:

$$P = P_j \exp - \left[ \frac{H_{vn}}{RT_j} \left( \frac{T_j}{T} - 1 \right) \right]$$

where  $H_{vn}$  is the latent heat of vaporization per mole of species  $n$ . It is found from tabulations of  $H_v$  for families of organic compounds that it is approximately constant, taken on a mass basis, or proportional to molecular weight, for a given family. The vapor pressure of a polymer fragment of size  $n$  is then expressible as

$$P_n = P_{jn} \exp - \left[ \frac{n H_{vm}}{RT_j} \left( \frac{T_j}{T} - 1 \right) \right] \quad (32)$$

With Equation 22, this gives

$$P_c = \sum_{n=N_{\min}}^N P_{jn} \exp - \left[ \frac{n H_{vm}}{RT_j} \left( \frac{T_j}{T_w} - 1 \right) \right] \quad (33)$$

where  $H_{vm}$  is the molar heat of vaporization of the monomer.

Combustion chamber pressure must be regarded as being set independently of the fuel pyrolysis processes. Also, the interface temperature  $T_w$  is to some extent defined experimentally. Arbitrary selection of a  $T_w$  and  $P_c$  results in general in Equation(33)not being satisfied. Summing to one minimum fragment size leads to pressure less than  $P_c$ , while the next smaller  $N_{\min}$  results in an excess polymer vapor pressure. Two means of avoiding this difficulty can be considered. Vapor pressure equilibrium may be assumed for all fragment sizes greater than  $N_{\min}$ ,

with its vapor pressure contribution just sufficient to sum to  $P_c$ . This implies that the fragment of size  $n = N_{\min}$  vaporizes at a rate controlled solely by the kinetic rate of its production. Alternatively, it could be assumed that all fragment sizes including the smallest allowed are in vapor pressure equilibrium, and that Equation(33) is satisfied by permitting  $T_w$  to float over a small range. These choices must be considered with reference to an energy equation and the kinetic rate equation.

The assumption of vapor pressure equilibrium between the gas phase polymer fragments and condensed phase leads to a further problem. The mass flux of gas from the surface is equal to  $\rho_F \dot{r}$ , and, in terms of fragment vapor pressures, this is

$$\begin{aligned} \rho_F \dot{r} &= V_w \sum_n \rho_n \\ &= V_w \frac{M}{RT_w} \sum_n n P_{jn} \exp - \left[ \frac{nH_{vm}}{RT_j} \left( \frac{T_j}{T} - 1 \right) \right] \end{aligned}$$

This then imposes a requirement on the relative vaporization rates of the various fragment sizes, and hence on the composition of the degraded polymer at the phase change interface. In order that such a composition exists there, in general it must be assumed that fragments migrate by diffusion within the polymer. This mechanism, although not necessarily unimportant, has not been included in the polymer degradation model.

The overall energy balance for a pyrolyzing material is commonly written as

$$\dot{q}_w = \rho_F \dot{r} h_p$$

(34)



and the quantity  $h_p$  treated as a constant. It is clear from the preceding discussion, however, that  $h_p$  is in fact coupled with the vaporizing fragment size and interface temperature. It is here expressed as

$$\begin{aligned} h_p &= c (T_w - T_i) + \left(1 - \frac{I_w}{I_o}\right) H + \frac{H_{vm}}{M_m} \\ &= c (T_w - T_i) + \frac{H}{N_w} + \frac{H_{vm}}{M_m} \end{aligned} \quad (35)$$

A first question of interest is whether the full set of equations describing polymer degradation and the matching conditions has a real solution. Examination of them does indicate that a priori specification of  $P_c$  and  $\dot{q}_w$  does lead to a unique  $T_w$  and  $\dot{r}$ , as well as a vaporizing fragment size distribution. The question of whether the smallest fragment included gives its full vapor pressure at  $T_w$ , or only that fraction sufficient to provide the assigned  $P_c$ , has not been answered.

Pyrolysis of all polymer as monomer is, as noted above, kinetically feasible with the subject analysis, if the alternative interpretation<sup>(13, 19)</sup> of  $N_w$  is taken. The energy balance for the polymer surface, Equations 34 and 35, is clearly affected, however. The effective heat of pyrolysis is about 80% greater for PMMA monomer than for trimer, at a specified wall temperature. Since in conventional turbulent heat transfer models  $h_p$  appears only in the thermochemical parameter  $B$ , which itself appears as  $B^{0.23}$ , assuming trimer rather than monomer pyrolysis leads to only a fifteen percent increment in calculated  $\dot{r}$ . The actual vaporizing fragment size is thus not too significant in the energy transport model.

Choice of monomer as pyrolysis product, rather than the kinetically effective fragment sizes, requires a different interpretation of pressure matching conditions. It is readily shown that the vapor pressure of methyl methacrylate at real wall temperatures is appreciably higher than any combustion pressure of interest. The assumption of vapor pressure equilibrium is therefore clearly not tenable. It must be assumed that monomer vapor pressure approximates combustion pressure, at

the wall, and that monomer vaporizes essentially as fast as produced, while larger fragment sizes remain in the condensed phase until broken.\*

In general, this is a simpler mathematical system than is the case of large fragment vapor pressure equilibrium. Specification of  $T_w$  and an effective fragment size defines  $\dot{r}$ . The linear pyrolysis rate and wall temperature, in the energy matching condition, give a requisite heat flux to the wall.

---

\* It is recognized that small fragments, with finite vapor pressure, contribute a small amount to the fuel vaporization rate.

REFERENCES

1. Lutz, O., "Vergleichsbetrachtungen und Treibstofffragen bei R-Antreiben," Akademie für Luftfahrtforschungen 37, 13-14, (1943).
2. Bartel, H. R., and Rannie, W. D., Solid Fuel Combustion as Applied to Ramjets, Progress Report 3-12, Jet Propulsion Laboratory, California Institute of Technology, 1946.
3. Marxman, G., and Gilbert, M., Ninth Symposium (International) on Combustion, ed. by W. G. Berl (Academic Press, New York, 1963) pp.371-383.
4. Marxman, G. A., Wooldridge, C. E., and Muzzy, R. J., "Fundamentals of Hybrid Boundary Layer Combustion," Progress in Aeronautics and Astronautics, Vol.15, Academic Press, New York (1964).
5. Investigation of Fundamental Phenomena in Hybrid Propulsion, Vol.1, Final Technical Report, Nov. 1965, United Technology Center, Sunnyvale, Calif.
6. Smoot, L. D., and Price, C. F., "Regression Rate Mechanisms of Non-Metallized Hybrid Fuel Systems," AIAA Preprint 65-56 (1965).
7. Smoot, L. D., and Price, C. F., "Regression Rates of Metallized Hybrid Fuel Systems," AIAA IV, 5, May 1966 pp.910-915.
8. Kosdon, F. J., and Williams, F. A., "Pressure Dependence of Non-metallized Hybrid Fuel Regression Rates," AIAA J. V 4, April 1967 pp.774-778.
9. Smoot, L. D., Price, C. F., "Pressure Dependence of Hybrid Fuel Regression Rates," AIAA J. V 1, January 1967 pp.102-106.
10. Wooldridge, C. E. and Marxman, G. A., "A Simple Regression Rate Model for the Pressure-Sensitive Domain of Hybrid Combustion," Western State Section-Combustion Institute Paper No.68-22.
11. Rabinovitch, B., "Regression Rates and the Kinetics of Polymer Degradation," Tenth Symposium (International) on Combustion, The Combustion Institute, 1965 pp.1395-1404.
12. Houser, T. J., and Peck, M. V., "Research in Hybrid Combustion," Progress in Aeronautics and Astronautics, Vol. 15 Academic Press, New York (1964).
13. Nagler, R. G., "Degradation of Homogeneous Polymeric Materials Exposed to High Heat Fluxes," Jet Propulsion Laboratory, California Institute of Technology, Technical Report No. 32-527, February 1964.
14. Anderson, R., Brown, R. S., Thompson, G. T., and Ebeling, R. W., "Theory of Hypergolic Ignition of Solid Materials," Internal Report, United Technology Center, Sunnyvale, California.

15. Cohen, S., "Aspects of Heterogeneous Combustion above a Flat Plexiglas Slab," S. M. Thesis, Chemical Engineering Dept., M.I.T., August 1968.
16. Muzzy, R. J., "Mixing within a Turbulent Boundary Layer with Surface Mass Addition," Engineers Thesis, Stanford University, May 1966.
17. Vranos, A., Faucher, J. E., and Curtis, W. E., "Turbulent Mass Transport and Rates of Reaction in a Confined Hydrogen-Air Diffusion Flame," Twelfth Symposium (International) on Combustion, The Combustion Institute, 1969 pp.1051-1057.
18. Guenther, R., and Simon, H., Twelfth Symposium (International) on Combustion, The Combustion Institute, 1969, pp.1069-1079.
19. Madorsky, S. L., Thermal Degradation of Organic Polymers, Interscience, New York, 1964, pp.179, 180.
20. Grassie, N., and Melville, H. W., "The Thermal Degradation of Polyvinyl Compounds," Proceedings of the Royal Society, London, A 199 October 1949.
21. Chaiken, R. F., Anderson, W. H., Barsh, M. K., Mishuck, E., Moe, G., and Schultz, R. D., "Kinetics of the Surface Degradation of Polymethylmethacrylate," Journal of Chemical Physics Vol. 32 No. 1 Jan. 1960 pp.141-146.
22. McAlevy, R. F., Lee, S. Y. and Smith, W. H., "Linear Pyrolysis of Polymethylmethacrylate during Combustion," AIAA J. VI, 6 June 1968 pp.1137-1142.
23. McAlevy, R. F., and Hansel, J. G., "The Linear Pyrolysis of Thermoplastics in Chemically Reactive Environments," AIAA Preprint 64-86.
24. Marxman, G. A., Tenth Symposium (International) on Combustion, p.1337, The Combustion Institute, 1965.
25. Wooldridge, C.E., and Muzzy, R., "Boundary Layer Turbulence Measurements with Mass Addition and Combustion," Tenth Symposium (International) on Combustion, p.1337, The Combustion Institute, 1965.
26. Rosenfeld, J.L., and Sugden, T.M., Combustion and Flame 8, Vol. 37, 1964.

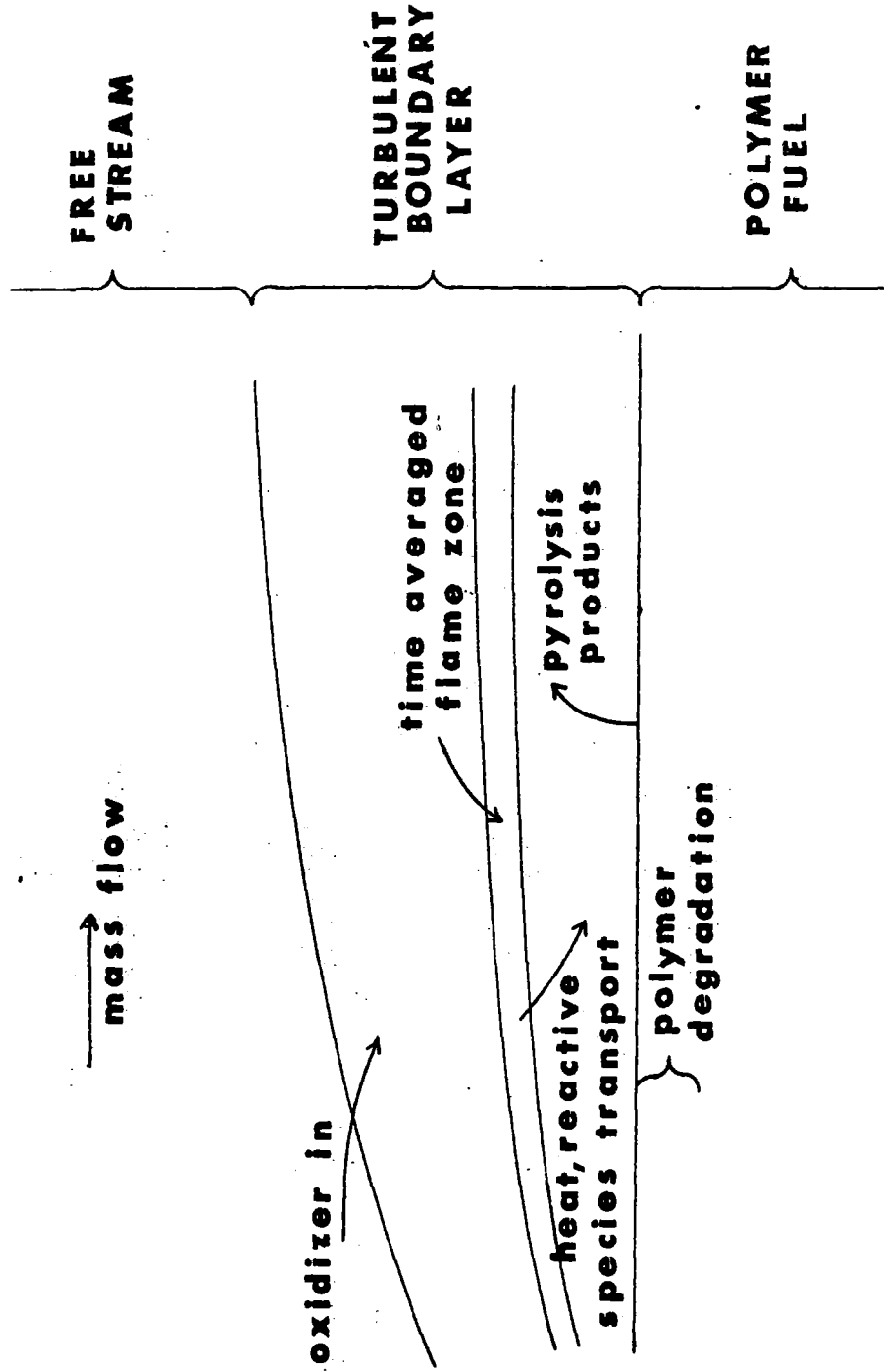


FIG. 1 TURBULENT BOUNDARY LAYER COMBUSTION FORMAT

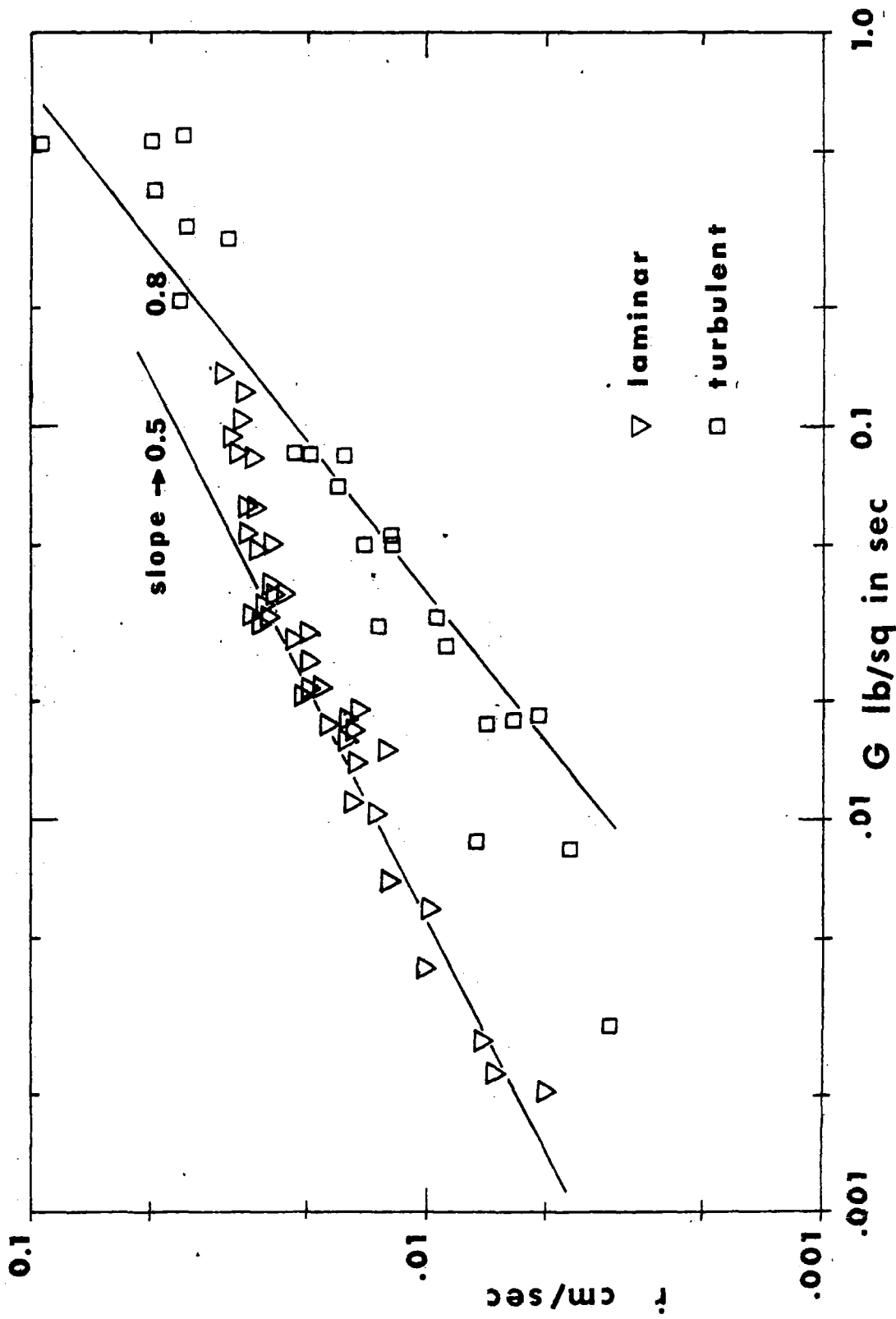
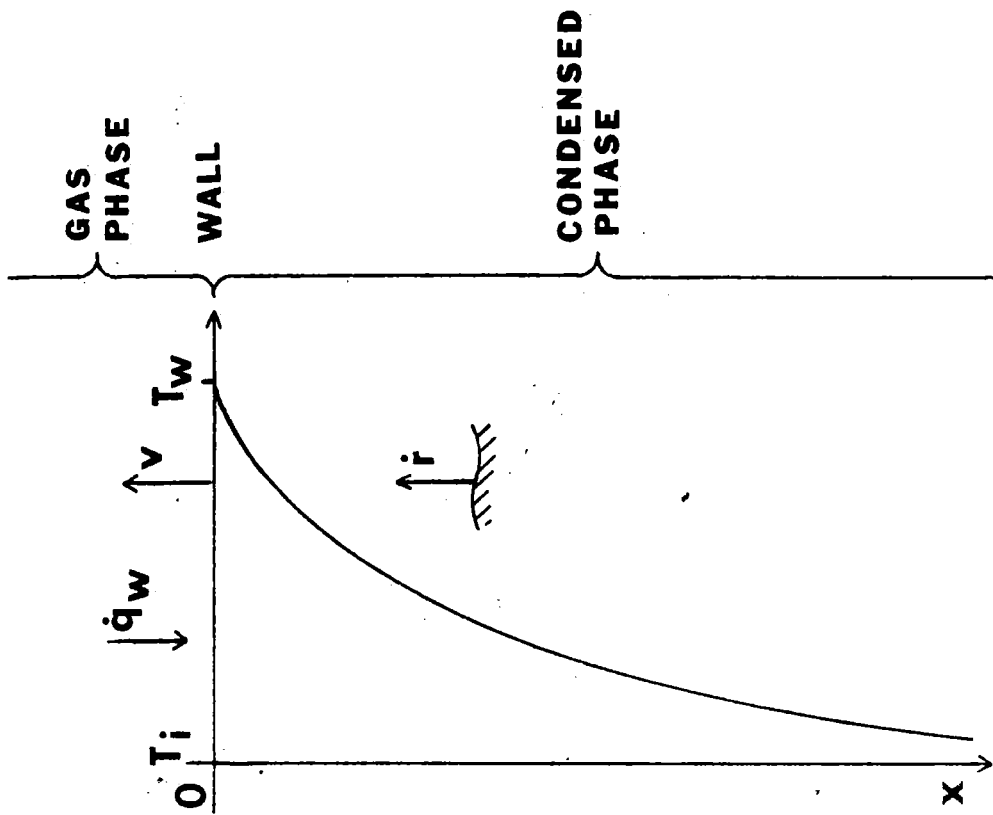
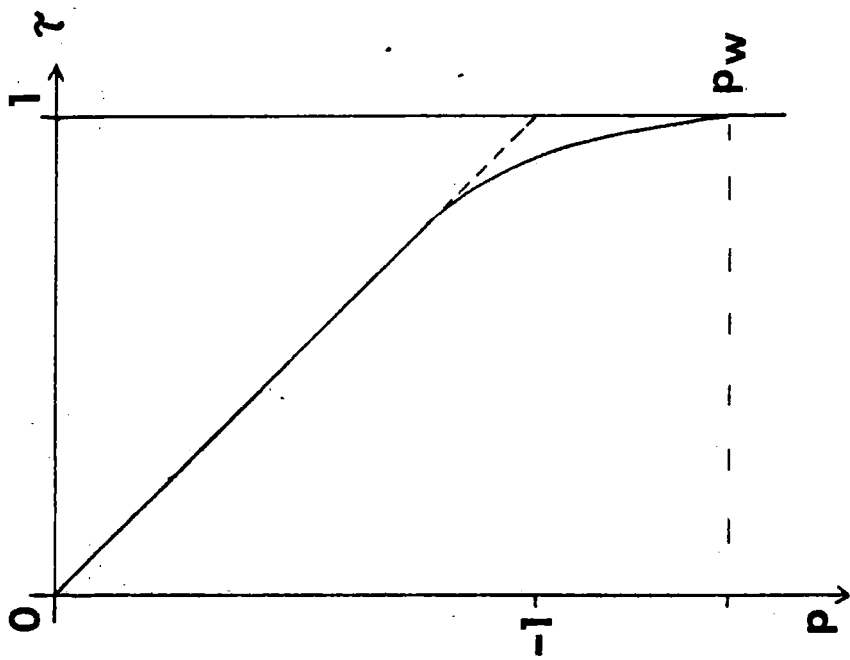


FIG. 2 POLYMER REGRESSION RATE DEPENDENCE ON FREE STREAM MASS VELOCITY



**FIG.3 POLYMER DEGRADATION REGION GEOMETRY**



**FIG.4 DIMENSIONLESS VARIABLE SOLUTION CURVE**

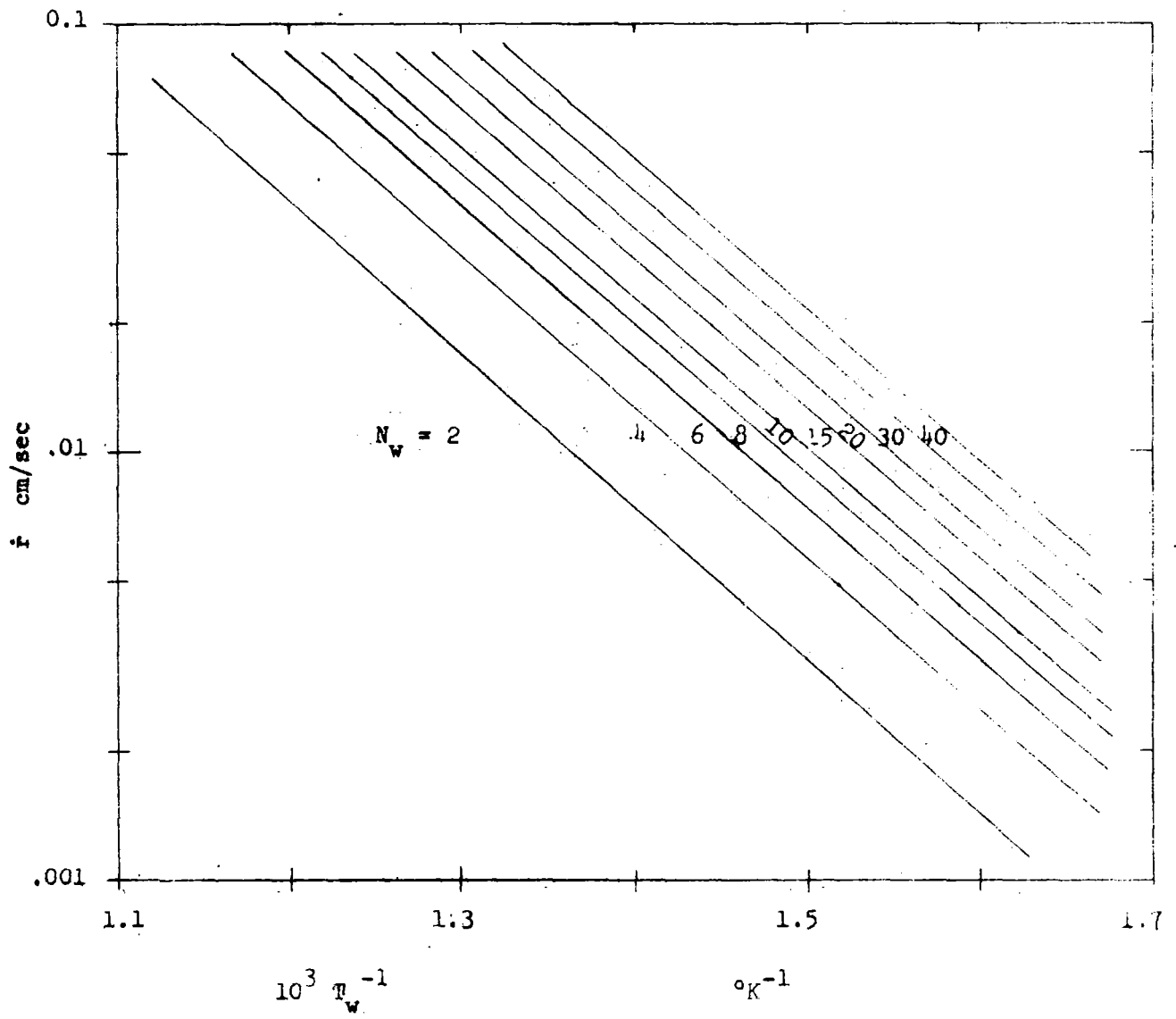


FIG. 5 CALCULATED POLYMER PYROLYSIS RATE  
ANALYTIC SOLUTION, ACTIVATION ENERGY CONSTANT



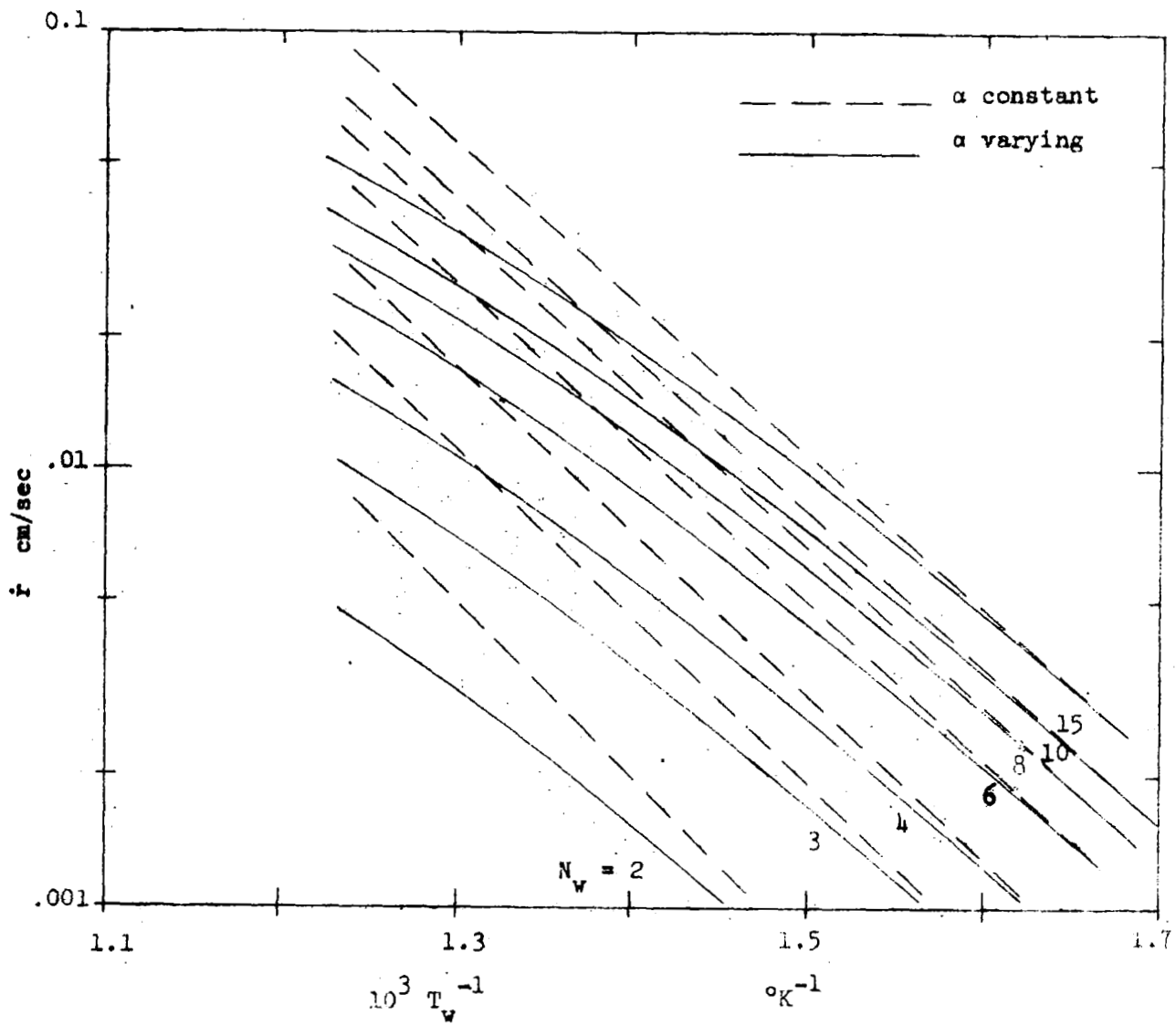


FIG. 6 CALCULATED POLYMER PYROLYSIS RATE  
 NUMERICAL SOLUTION FOR PMMA, WITH VARYING ACTIVATION ENERGY

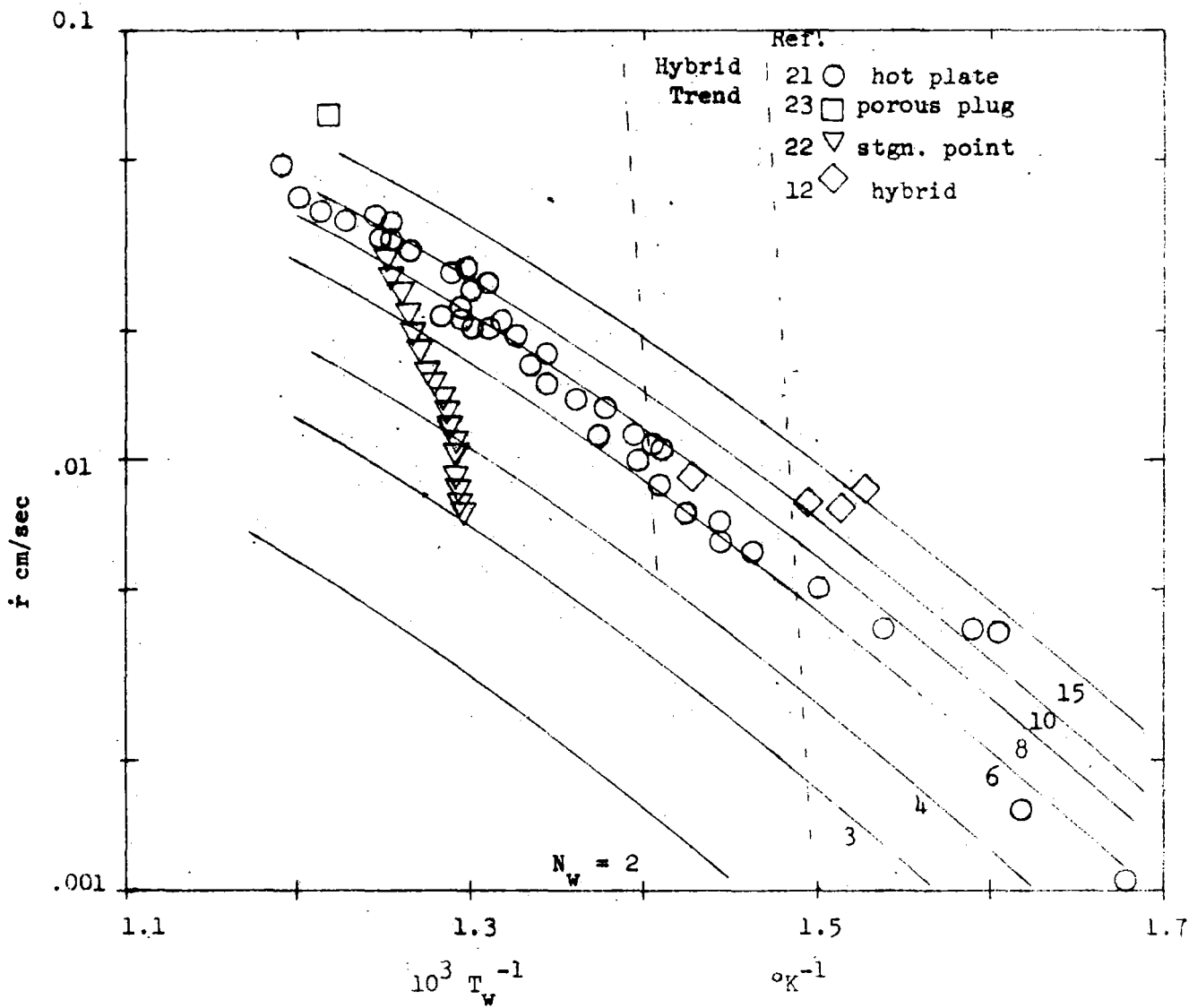


FIG. 7 POLYMER PYROLYSIS RATE; PMMA  
SOLID LINES - VARYING  $E$ ,  $\alpha$  SOLUTION

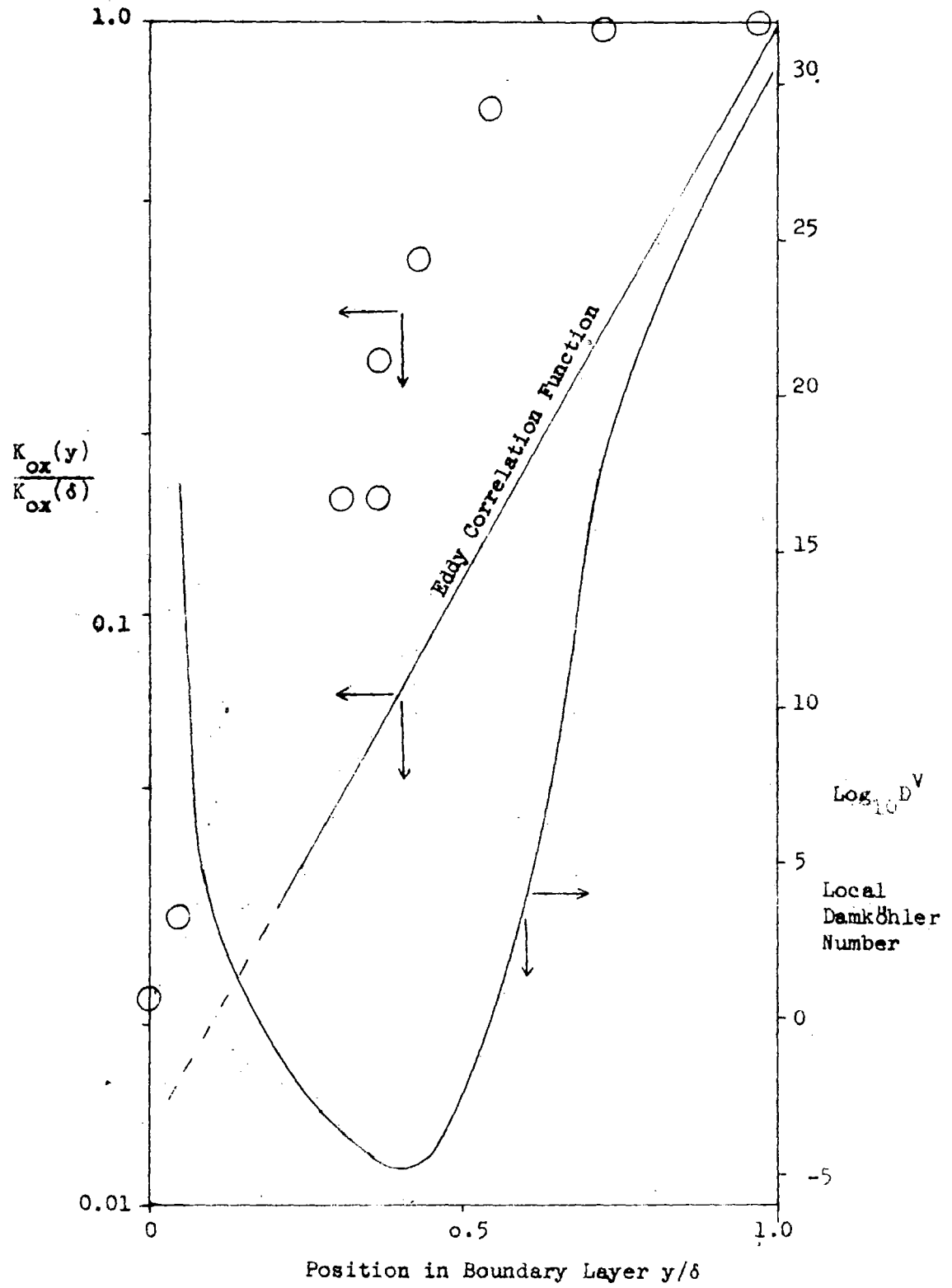


FIG. 8 TURBULENT MIXING AND REACTION IN HYBRID BOUNDARY LAYER